

Memorandum

To: CSC Distribution
From: F. Primini
Date: 04/27/2012
Subject: Limiting Sensitivity Specification

1 Introduction

Limiting Sensitivity describes quantitatively the power of our detection procedure to detect faint sources. Typically, point source detection relies on a test statistic, S , which is a function of source and background counts, PSF , and the statistical noise model in a region around the putative source. A source is said to be detected if S exceeds the detection threshold, S^* . Determining Limiting Sensitivity then reduces to determining, at each location in the image, the value of the source counts that would yield $S = S^*$ at that location. In general, this depends on the local background, PSF , and S^* .

For the CSC Release 1, the test statistic used was SNR , the ratio of the maximum likelihood estimates for net source counts and error (see, e.g., equations 15-17 of Evans et al. 2010). Background estimates were derived from a model background map, randomized with Poisson statistics. A main advantage of the Release 1 algorithm was that it depended on the PSF only through its integrals in source and background apertures, which could be estimated easily from calibration data without generating actual $PSFs$ at each image location. Moreover, the formula for SNR could be solved easily to yield the net counts for which $SNR = SNR^*$.

For Release 2, the detection procedure is similar to that used in the $2XMM$ catalog (Watson et al., 2009), and a different test statistic is used. For each source candidate identified by wavdetect, two 2-dimensional spatial models are fit to the image data - one consisting of background only, and the other of background plus a point source convolved with the PSF . The best-fit C -statistic for each model is computed and the probability P of obtaining an increase in C at least as large as that observed, in the absence of a real source, is evaluated. The test statistic is the Likelihood L (actually the log-Likelihood), defined as $L = -\ln P$; if the wavdetect candidate is not due to background fluctuations, P should be small (L large) and the source is detected if $L \geq L^*$. The threshold L^* is expected to depend on off-axis angle and will be determined through simulations.

Unlike the case in Release 1, a detailed knowledge of the PSF is required to calculate the best-fit C for the point source model, and hence to determine the Limiting Sensitivity. Moreover, there is no simple algebraic solution for net counts at which $L = L^*$. Fortunately, an alternative approximate solution is available based on a simple empirical relationship between L and net source counts for detected sources. This relationship can be extrapolated to determine net counts at detection threshold. This will form the basis of the Release 2 Limiting Sensitivity algorithm.

2 Algorithm

The empirical relationship between L and net source counts formed the basis of the $2XMM$ sensitivity maps, and since our detection procedure is similar, it should apply here as well. The algorithm is described in detail in Appendix A of Carrera et al. (2007), who noted that for sources detected with likelihood L , there was a linear relationship between the $2XMM$ count rate R and the quantity $crpoisim$, determined from

$$-\ln(P(N \geq B + crpoisim \times expmap | B)) = L. \quad (1)$$

Here, $P(N \geq M | B)$ is the cumulative Poisson probability of obtaining M or more counts in a source aperture if the average background in the aperture is B , $expmap$ is the average exposure map value in the aperture, and the quantity $crpoisim \times expmap = ctpoisim$ has units of counts.¹ The cumulative Poisson probability is given by

$$P(N \geq B + ctpoisim | B) = \gamma(B + ctpoisim, B) \quad (2)$$

where the incomplete gamma function $\gamma(a, x)$ is defined as

$$\gamma(a, x) = \frac{1}{\Gamma(a)} \int_0^x e^{-t} t^{a-1} dt \quad (3)$$

(see sections 6.5 and 26.4 of Abramowitz & Stegun, 1970). The quantity $ctpoisim$ is then determined by finding the root of the equation

$$L + \ln(\gamma(B + ctpoisim, B)) = 0. \quad (4)$$

A plot of $L + \ln(\gamma(B + n, B))$ vs. n is shown in Figure 1 for two sample values of L and B . The function varies smoothly with n and its root should be easily determined numerically.

Using results from an *MLE* simulation of a 3-obsid cohort in M17, I have verified that the correlation between net source counts and $ctpoisim$ reported in Carrera et al. (2007) also holds for our *MLE* procedure (actually, they reported a correlation between net rate and $crpoisim$, but the conversion between counts and rate is the same for both quantities). I used b band fitted background counts in sources apertures and detected source likelihoods reported by *MLE* to compute $ctpoisim$, and compared these values to the net source counts reported by *MLE*. The results are shown in Figures 2-5 and indicate a strong correlation both for sources detected in individual obsids and in the cohort (stacked obsids).

The procedure for determining Limiting Sensitivity then amounts to determining background B and average exposure map value E in a source aperture appropriate to the desired location, and to use B and the appropriate detection likelihood threshold L^* to determine $ctpoisim$ by finding the root to Equation 4. $crpoisim$ is then computed from $ctpoisim$ and E , and the empirical relation between $crpoisim$ and actual source photon flux, appropriate to the energy band and location, is then used to compute Limiting Sensitivity. Details of the empirical relation will need to be calibrated through simulations.

3 Specification

Limiting Sensitivity will be calculated for each stack, and for each energy band. Resolution of the input and output maps will be $4''$ (TBR). Since the simulations required to calibrate the $crpoisim$ relations have not yet been done, the output maps will be maps of $crpoisim$, and computation of the actual sensitivity maps from these will be deferred to a later step. HealPix tiling will also be deferred to a later step.

Certain quantities, such as source aperture size, or coefficients of the $crpoisim$ relations, depend on off-axis angle θ . Calculation of these quantities for a stack may be difficult since obsids in a stack may have different aimpoints, and hence there will be no unique θ for a given stack location. An average aperture size will be calculated at each location in the stack from the background-weighted aperture sizes at the corresponding locations of the individual obsids comprising the stack.² It is not clear how strongly the $crpoisim$ coefficients

¹For *2XMM*, $expmap$ and $crpoisim$ have units of time and count rate, respectively. In our case, the units are $cm^2 - s - count - photon^{-1}$ and $photon - cm^{-2} - s^{-1}$. In either case, $ctpoisim = crpoisim \times expmap$ has units of counts.

²An alternative weighting, using exposure rather than background, is also possible. This issue is TBR. For the remainder of this specification, background-weighting is assumed.

will depend on θ , so it's difficult to say at present whether variation in θ will be an issue. For convenience in later steps, maps of average, background-weighted θ values and the range of θ will also be computed.

3.1 Inputs

- model background map for each energy band for the stack and for individual obsids in the stack;
- exposure map for each energy band for the stack;
- 90% encircled energy *PSF* map for each energy band for each obsid in the stack;
- Likelihood threshold (L^*) map or maps for the stack; the L^* map may be a single value, or may vary with θ , and hence be expressed as an actual map; multiple thresholds, corresponding to different levels of source credibility, may be used (TBD); each would result in a different sensitivity map;

3.2 Outputs

- map of *crpoisim* values for each energy band for the stack, at the same resolution as the input maps; if multiple L^* maps are input, a *crpoisim* map will be produced for each;
- map of average off-axis angle $\bar{\theta}$, θ_{min} , and θ_{max} , at the same resolution as the input maps (for convenience for later determination of *crpoisim* coefficients).

3.3 Step-by-step Procedure

The following steps should be carried out for each energy band and for each logical pixel ($4'' \times 4''$, TBR) in the field-of-view of the stack:

1. Compute the average 90% encircled energy radius \bar{r}_{90} , according to

$$\bar{r}_{90} = \frac{\sum b_i \times r_{90,i}}{\sum b_i},$$

where b_i is the background map value and $r_{90,i}$ is the *PSF* map value at the corresponding location of the i^{th} obsid of the stack.

2. Compute the sum B of values in the background map stack within a circle of radius \bar{r}_{90} centered on the logical pixel.
3. Compute the simple average \bar{E} of values in the exposure map stack within a circle of radius \bar{r}_{90} centered on the logical pixel.
4. Determine the Likelihood threshold L^* at the corresponding location in the Likelihood threshold map.
5. Compute *ctpoisim* by finding the root to the equation $L^* + \ln(\gamma(B + ctpoisim, B)) = 0$.
6. Compute $crpoisim = ctpoisim / \bar{E}$.
7. Output map of *crpoisim* values.

If multiple threshold maps are available, steps 4-7 should be carried out for each map.

The following steps should be carried out once (*i.e.*, not for each energy band) for each logical pixel ($4'' \times 4''$, TBR) in the field-of-view of the stack:

1. Compute the average off-axis angle $\bar{\theta}$, according to

$$\bar{\theta} = \frac{\sum b_i \times \theta_i}{\sum b_i},$$

where b_i is the background map value and θ_i is the off-axis angle at the corresponding location of the i^{th} obsid of the stack.

2. Determine $\theta_{min} = \min(\theta_i)$ and $\theta_{max} = \max(\theta_i)$.
3. Output maps of $\bar{\theta}$, θ_{min} , and θ_{max} values.

4 Simulations

Simulations of point sources in stacks of ACIS-I, ACIS-S, and HRC observations will need to be carried out in order to calibrate the *crpoisim* correlations. Details of the simulations are TBR, but I anticipate they will be similar to those in current MLE simulations. Individual obsids in the stacks should span a range of exposures from 1-100 kiloseconds, and stacks should also include obsids with a range of exposures. Source densities in individual observations should vary with θ to ensure approximately uniform number of sources per θ bin, and sufficiently low in each simulation to avoid overlapping sources. Source intensities should span a range of intensities, down to ~ 5 counts per source on axis, and should be weighted to emphasize low-count sources. The total number of sources per θ bin should be $\gtrsim 100$ (TBR).

Each simulation should include all data and metadata necessary to run the CSC pipelines through *MLE*. Source output (source and background apertures, Likelihoods of detected sources, and backgrounds in source regions) from *MLE* will be collected, and the *NAP* aperture photometry tool will be run manually to determine photon fluxes of detected sources. Corresponding values of *crpoisim* will be calculated from the *MLE* output, and the photon flux/*crpoisim* pairs will be used to calibrate the *crpoisim* relations.

References

- Abramowitz, M., & Stegun, I. A., 1970, Handbook of mathematical functions : with formulas, graphs, and mathematical tables
- Carrera, F. J., et al., 2007, A&A, 469, 27
- Evans, I. N., et al., 2010, ApJS, 189, 37
- Watson, M. G., et al., 2009, A&A, 493, 339

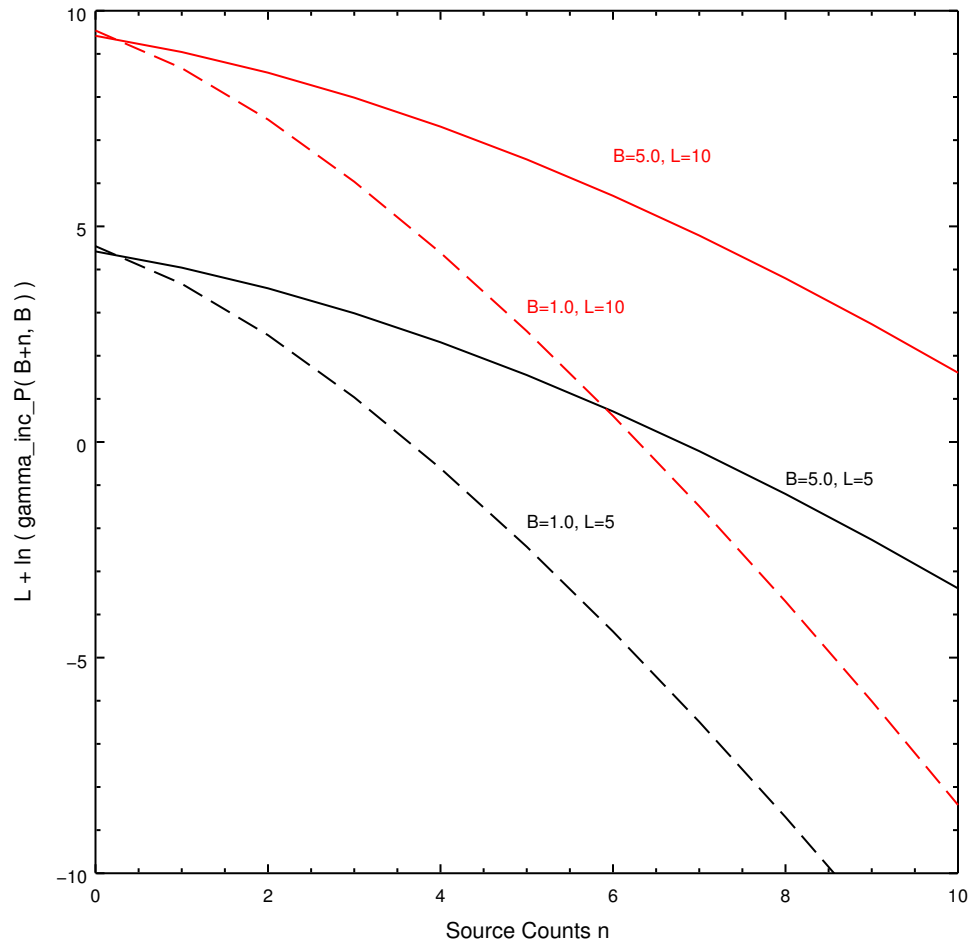


Figure 1: The function $L + \ln(\gamma(B + n, B))$ varies smoothly with n and has a single root which can be easily determined numerically.

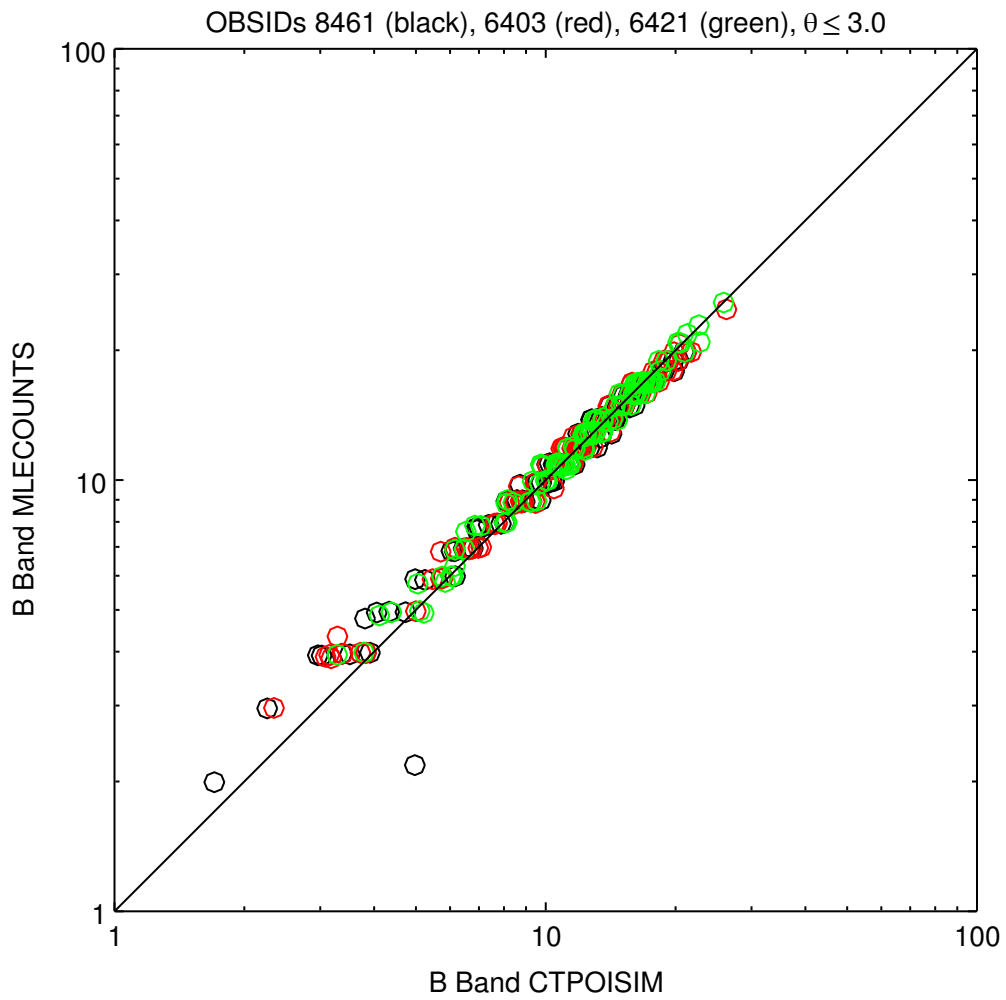


Figure 2: *MLE* counts vs. *ctpoisim* for sources with off-axis angles $\theta \leq 3'$.

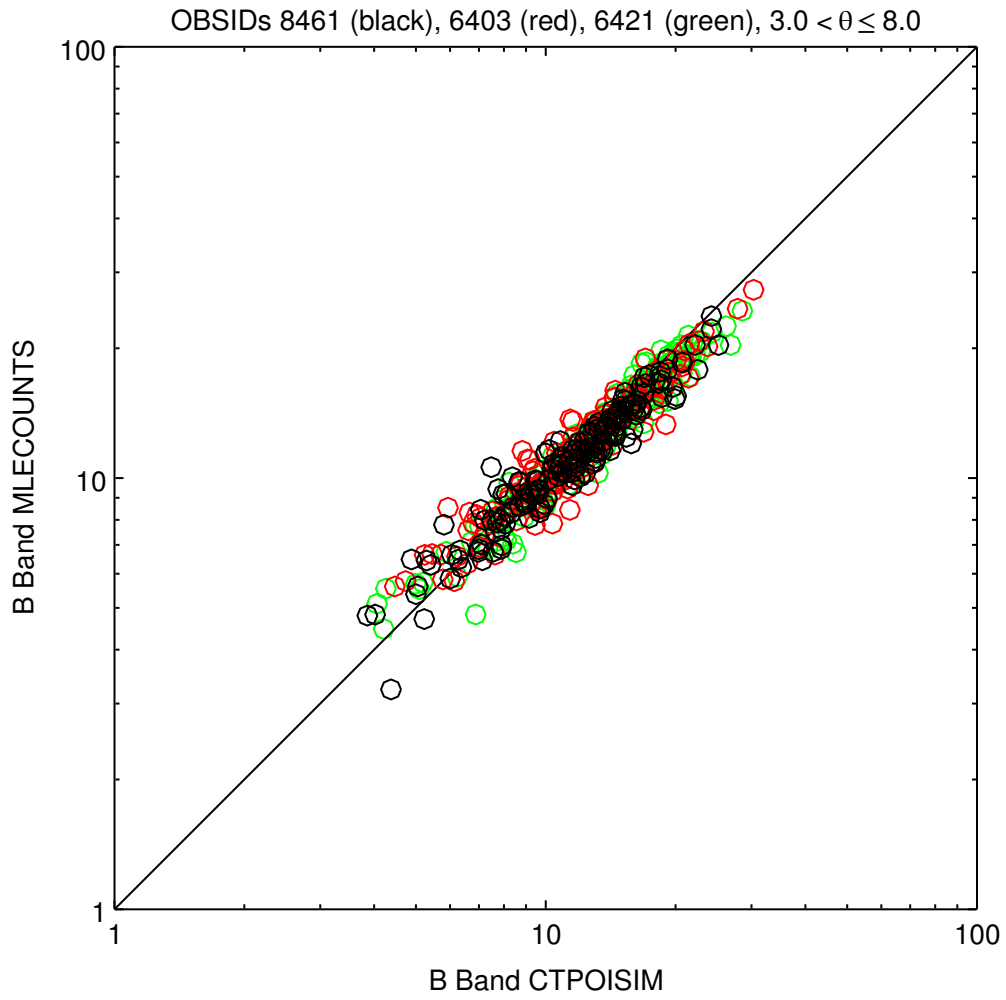


Figure 3: *MLE* counts vs. *ctpoisim* for sources with off-axis angles $3' < \theta \leq 8'$.

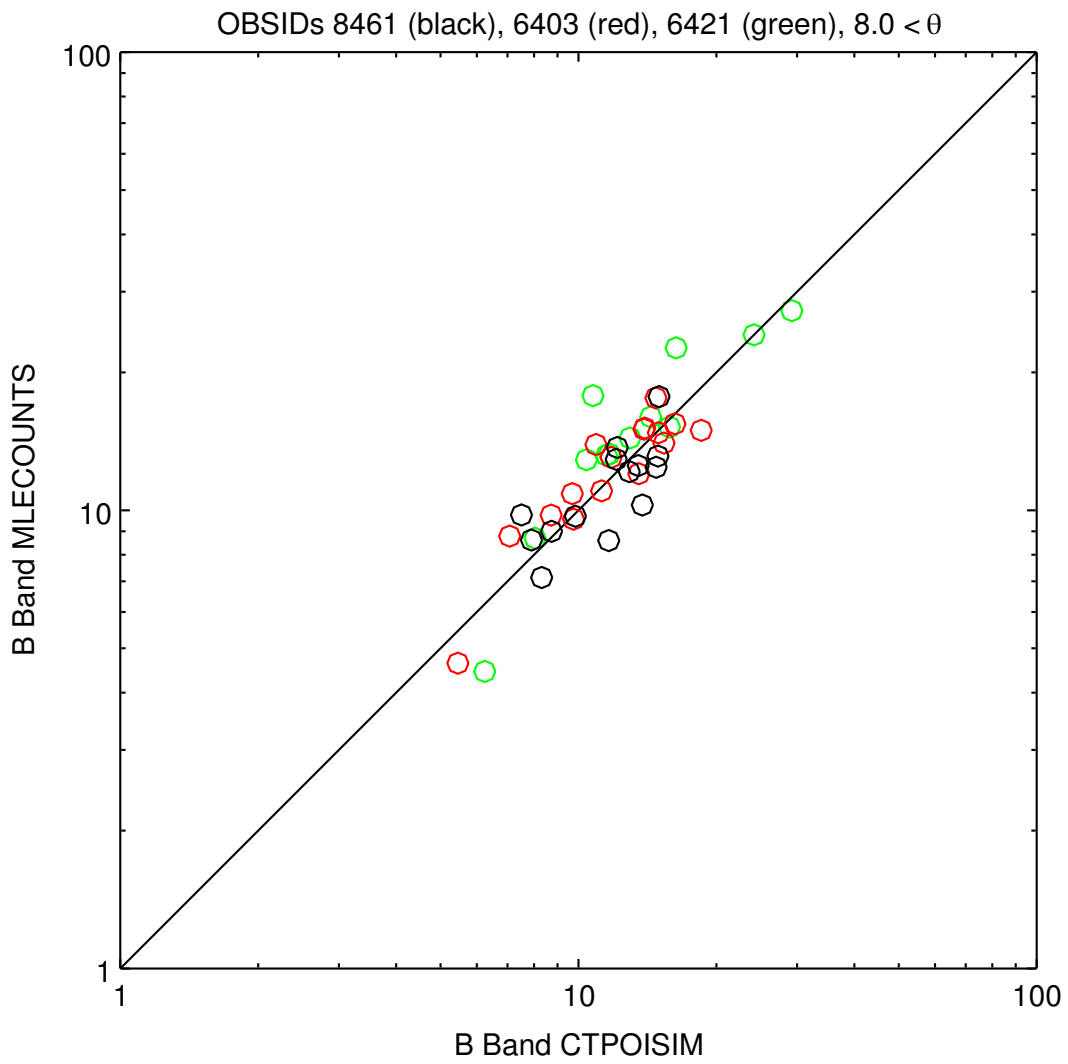


Figure 4: *MLE* counts vs. *ctpoisim* for sources with off-axis angles $\theta > 8'$.

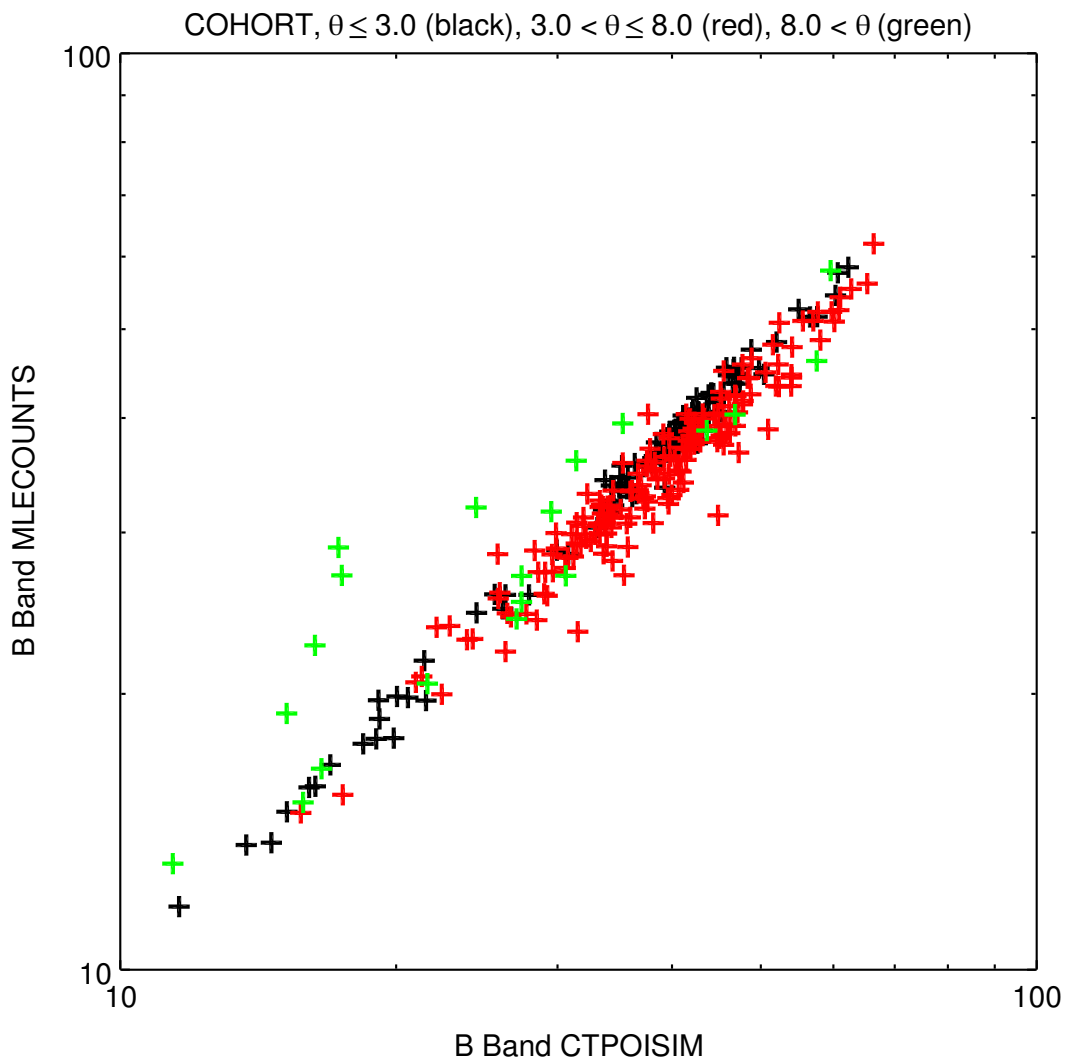


Figure 5: *MLE* counts vs. *ctpoisim* for sources detected in the cohort (stacked obsids).